OPEN ACCESS
IOP PUBLISHING
SCIENCE AND TECHNOLOGY OF ADVANCED MATERIALS
Sci. Technol. Adv. Mater. **14** (2013) 045004 (7pp)
doi:10.1088/1468-6996/14/4/045004

Anisotropic mobility and carrier dynamics in the β-type BEDT-TTF salts as studied by inter-layer transverse magnetoresistance

Shigeharu Sugawara and Masafumi Tamura

Department of Physics, Faculty of Science and Technology, Tokyo University of Science, Yamazaki 2641, Noda, Chiba 278-8510, Japan

E-mail: suga@rs.tus.ac.jp

Received 8 April 2013
Accepted for publication 24 June 2013
Published 23 July 2013
Online at stacks.iop.org/STAM/14/045004

Abstract
A new method to estimate an in-plane conduction anisotropy in a quasi-two-dimensional (q2D) layered conductor by measuring the inter-layer transverse magnetoresistance is proposed. We applied this method to layered organic conductors β-(BEDT-TTF)$_2$X (BEDT-TTF = bis(ethylenedithio)tetrathiafulvalene, $C_{10}H_8S_8$; X = IBr_2, I_2Br) by applying magnetic field rotating within the basal plane at 4.2 K. We found the anisotropic behaviour of carrier mobility μ. From this, anomalous distribution of carrier lifetime τ on the Fermi surface is derived, by the use of Fermi surface data reported for the materials. Calculations of the non-uniform susceptibility $\chi_0(\boldsymbol{q})$ suggest that carrier scattering is enhanced at specific $\boldsymbol{k}$-points related to partial nesting of the Fermi surface. The present method is thus demonstrated to be an efficient experimental tool to elucidate anisotropic carrier dynamics in q2D conductors.

Keywords: magnetotransport, mobility, BEDT-TTF, Fermi surface, carrier dynamics

1. Introduction

For layered conducting materials of recent physical interest, containing transition metal oxides and oxide or organic conductors, the inter-layer resistance under magnetic field is sometimes adopted as a useful tool to investigate the electronic structures. The angle-dependent magnetoresistance oscillations (AMRO) [1, 2] are known to give Fermi wavenumber from the oscillatory dependence on the elevation angle of the applied field with respect to the layer of quasi-two-dimensional (q2D) metals. A method to obtain the Fermi surface (FS) of organic conductors by AMRO has been already established [3]. An observation of the Shubnikov–de Haas oscillations clearly gives useful information, the cross-sectional areas of the FS. In the case of TMTSF salts (TMTSF = tetramethyltetraselenafulvalene, $C_{10}H_{12}Se_4$), peculiar angle dependence of transverse magnetoresistance (transverse MR) under high field has been shown to tell us the geometry of FS [4]. Once the shape of FS and the band structure are known, our next problem is to find the dynamical behaviour of carriers at each $\boldsymbol{k}$-point on the FS. Carrier scattering is obviously crucial for the transport phenomena, and it gives significant information on the interactions operating on FS. For this topic, Kontani and co-workers [5, 6] pointed out that there are so-called hot spots on the FS of some strongly correlating systems, where strong scattering effect arises due to correlation, and this feature brings about some anomalous transport properties. Such scattering effect specific to correlating carriers can be detected as anisotropic carrier lifetime (or relaxation time) τ [5]. The above-mentioned experiments, AMRO and the Shubnikov–de Haas effect, are based on the field component perpendicular to the plane, so that they only give the averaged value of the lifetime, for example, as the Dingle temperature.

Recently, we have devised a convenient method to investigate the anisotropic conduction by measuring the inter-layer transverse MR, which is the inter-layer resistance under transverse magnetic fields within the conduction plane. In previous studies [7, 8], transverse MR under weak magnetic fields has been confirmed to obey a simple equation

$$[R_\perp(B,\phi)/R_\perp(0)]^2 = 1 + \mu^2_{\phi\pm\pi/2}B^2, \quad (1)$$

where $R_\perp(B,\phi)$ is the inter-layer resistance under the in-plane field B applied for azimuth angle ϕ, $R_\perp(0)$ is the resistance at zero field and μ_α is the in-plane mobility of carriers moving in the $\alpha = \phi \pm \pi/2$ direction, perpendicular to the field. This is based on the Lorentz force applied by the in-plane field to the current perpendicular to the plane, $\boldsymbol{I}_\perp \times \boldsymbol{B}$, which induces the in-plane component of current perpendicular to the field, so as to yield transverse MR. Applying this to the experimental transverse MR data with the field rotating within the plane, we can obtain the mobility as a function of in-plane azimuth direction, $\alpha = \phi \pm \pi/2$. In other words, transverse MR experiments give information equivalent to that from dc resistivity measurements for various in-plane current directions, α. Experimentally, it is a difficult task to control dc current direction in a small specimen. Although the ac current direction is controllable by the use of microwave or infrared light polarization, wide-range frequency dependence is required to evaluate physical parameters such as mobilities. Since the field direction can be easily controlled, this transverse MR measurement contrastingly provides the most convenient way to regulate the dc current direction to give direct information on anisotropic conduction in the layer.

In a previous paper [8], the shapes of FS of organic superconductors, κ-(BEDT-TSF)$_2$FeX$'_4$ (BEDT-TSF = bis(ethylenedithio)tetraselenafulvalene, $C_{10}H_8S_4Se_4$; X$'$ = Cl, Br), were inferred from the inter-layer TMR results to compare with those concluded from the AMRO and band calculations [9–11], as a check of consistency. The agreement was, however, not satisfactory; a remarkable discrepancy was found. In [8], uniform and $\boldsymbol{k}$-independent lifetime τ of carriers on an elliptic FS of nearly free 2D electrons was assumed. In this case, the anisotropy of μ is prescribed only by the anisotropy of the band structure, which leads to $\mu_\alpha = |e|\tau/\langle m^*_\alpha\rangle \propto 1/k^2_{\mathrm{F}\alpha}$, where $\langle m^*_\alpha\rangle$ is the α-component of the effective mass and $k_{\mathrm{F}\alpha}$ the Fermi wavenumber for the α-direction. The shape of FS, as described by $k_{\mathrm{F}\alpha}$, was thus estimated simply from the μ_α data [8]. The discrepancy suggests that $\mu_\alpha \propto 1/k^2_{\mathrm{F}\alpha}$ is not appropriate because of the $\boldsymbol{k}$-dependent τ. The mobility should be considerably affected by the distribution of lifetime τ on FS. It then turns out that the transverse MR is applicable to evaluate the distribution of τ, when combined with reliable data on the band structure and FS. We surmise here that the information on dynamical behaviour of the carriers on FS, which is to be distinguished from the static anisotropy of FS, can be extracted from transverse MR data.

In this work, a formulation is revised to obtain the scattering dynamics in a general band model for this purpose. The mobility appearing in equation (1) is explicitly written as a kind of weighted average of the component of the Fermi velocity $(v_{\mathrm{F}})_\alpha$, instead of using the elliptic FS model, which is too coarse particularly near the Brillouin zone boundary. We can thus estimate the distribution of the lifetime (or scattering rate) of each $\boldsymbol{k}$-point on FS. This information is rarely obtained by other types of transport measurements.

In this paper, the inter-layer transverse MR method is applied to examine the anisotropic in-plane conduction and the scattering dynamics on FS in q2D organic conductors β-(BEDT-TTF)$_2$X (X = IBr_2, I_2Br) [12, 13]. These two salts, having almost identical structures, are chosen in order to avoid superconductivity at 4.2 K, which prevents transverse MR from appearing under low field. The IBr_2 salt is reported to have $T_c = 2.7$ K or lower [12, 14], and the I_2Br salt does not exhibit superconductivity due to random orientation of the anions. The in-plane anisotropic behaviour of the mobility has been obtained from the transverse MR data collected at 4.2 K. From this, a peculiar distribution of the lifetime of carriers on FS has been derived. The results suggest two-carrier correlation at specific $\boldsymbol{k}$-points on the FS. To get insight into the origin of this correlation, we have calculated the static susceptibility, $\chi_0(\boldsymbol{q})$. The $\chi_0(\boldsymbol{q})$ map suggests that some $2\boldsymbol{k}_{\mathrm{F}}$ fluctuation modes are responsible for the carrier scattering.

2. Experimental

Plate-like single crystals of β-(BEDT-TTF)$_2$X (X = IBr_2, I_2Br) were grown by the electrochemical oxidation of BEDT-TTF in dichloromethane solutions containing $(n\text{-}C_4H_9)_4NX$. The dimensions of the samples were typically $0.5 \times 0.7 \times 0.2\,\mathrm{mm}^3$ (the IBr_2 salt) and $1.0 \times 0.8 \times 0.1\,\mathrm{mm}^3$ (the I_2Br salt). Pairs of Au wires were attached on both bc-faces of each sample by carbon paste, for the four-probe measurements of the inter-layer resistance. Inter-layer TMR data were collected at 4.2 K under magnetic field swept up to 7 T. The field $\boldsymbol{B}$ was rotated within the bc-plane by steps of about 8° (the IBr_2 salt) and 12° (the I_2Br salt) from $\phi = 0°$ to 240°, where $\phi = 0$ is directed to the b-axis. The experimental configuration of the transverse MR in this study is shown in the inset of figure 2(b). The crystal axes of the samples were checked by polarized infrared reflectance measurements at room temperature by the use of JASCO FT/IR-6100 equipped with a microscope, and related to the field angle. We refer to the definition of the crystal axes as used in [13], for both salts. (Note that k_b and k_c switch places in figure 5 of [13].)

3. Inter-layer transverse MR of β-(BEDT-TTF)$_2$X

Temperature dependence of the inter-layer resistance of these salts is metallic down to 4.2 K from room temperature. According to the in-plane resistance measurement [15], T^2-dependence $R(T) = R(0) + AT^2$ was observed in the range $T < 20$ K, where the quadratic term is due to electron–electron scattering. Such Fermi liquid behaviour is also observed in the inter-layer resistance below 30 K for both salts as shown in figure 1.

Field dependence of the inter-layer transverse MR at 4.2 K for several field angles ϕ measured from the b-axis is shown in figure 2, where the square of the inter-layer resistance normalized by the resistance at zero field is plotted

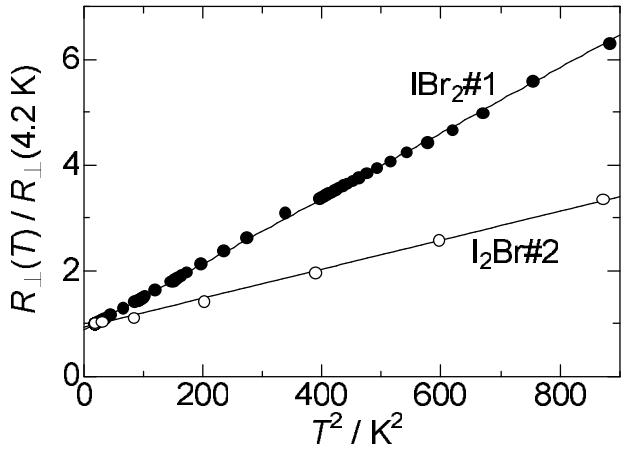

Figure 1. Temperature dependence of the inter-layer resistance of β-(BEDT-TTF)$_2$X (X = IBr$_2$, I$_2$Br). The resistance normalized by the value at 4.2 K is plotted versus the square of the temperature. Fermi liquid behaviour, $R_\perp(T) = R_\perp(0) + AT^2$, is observed.

versus B^2. For both salts, the transverse MR data exhibit linear dependence on B^2, obeying equation (1). ϕ-dependence of the transverse MR is qualitatively consistent with the experiment at 1.45 K under 15 T done by Kartsovnik *et al* [16]. In the earlier study [17], the anisotropic transverse MR under high field was discussed in terms of the curvature of FS on the basis of the equation of transverse MR derived by Lebed and Bagmet [4] where $\boldsymbol{k}$-independent τ is assumed. The anisotropy was qualitatively explained by FS curvature, but discrepancy still remains. In fact, in the present case, therefore, it is required to take account of the $\boldsymbol{k}$-dependence of τ, i.e. the anisotropic dynamics of carriers.

From the slope data in figure 2 as a function of ϕ, the mobility for the direction perpendicular to the field, $\mu_{\phi\pm\pi/2}$, is calculated. The obtained anisotropic mobility is plotted against $\alpha = \phi \pm \pi/2$ in figure 3. The information on the anisotropic in-plane conduction is thus summarized as the α-dependence of μ. The two salts exhibit similar angle dependence. Owing to anion disorder, the mobility of the I$_2$Br salt is about 1/5 times as low as that of the IBr$_2$ salt over the whole angle range.

The FS of the IBr$_2$ salt deduced from the AMRO data [3] is displayed in the inset of figure 3(a). As anticipated from its shape, the reciprocal effective mass $1/m^*$ is the smallest near c-direction ($\alpha = 110^\circ$). If τ is a uniform constant on FS, μ is expected to show a similar α-dependence. The observed anisotropy of μ shows this expected trend. However, the anisotropy of $1/m^*$ is not sufficiently large to yield the observed strong anisotropy of μ; the maximum to minimum ratio of μ amounts to about 3 for IBr$_2$ salt and 2.5 for I$_2$Br salt. (The minimum direction is slightly different between the two salts, probably due to a subtle difference in the crystal structures.) The results manifest that the anisotropy of μ not only involves the band structure but also is strongly affected by the anisotropic scattering dynamics in these materials. The α-dependence of μ indicates that the lifetime τ has particular k-dependence on FS considerably stronger than that of $1/m^*$. To explain the observed anisotropy of μ, τ should be considerably suppressed for the $\perp$[011] current direction.

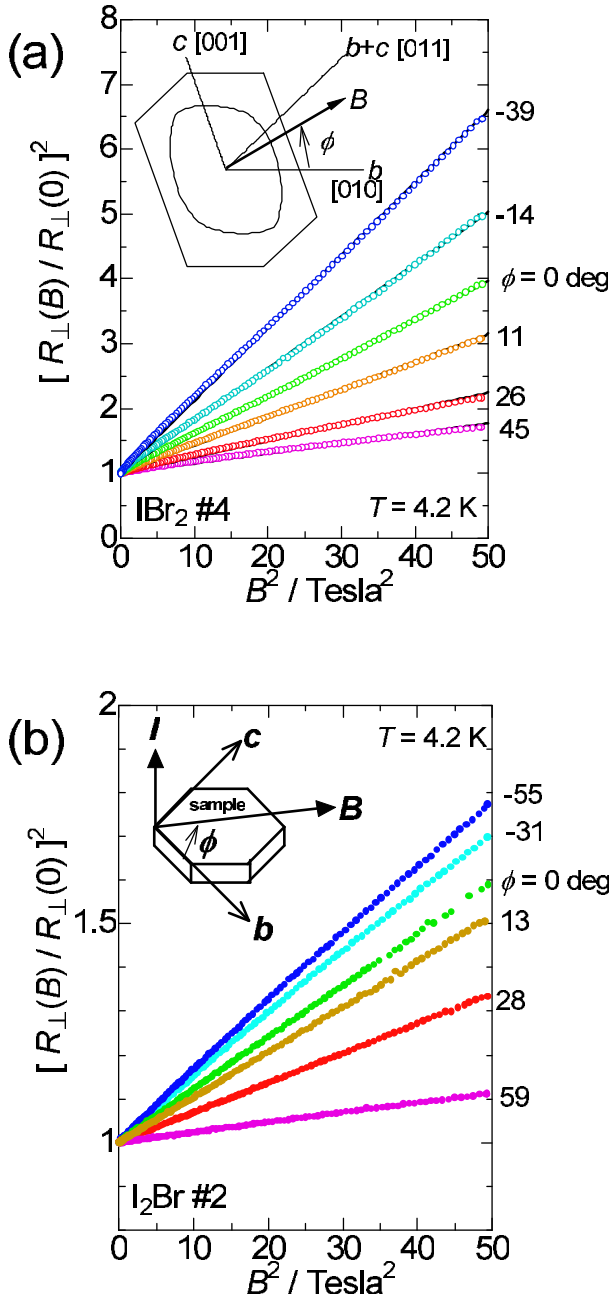

Figure 2. Field dependence of the inter-layer transverse MR of β-(BEDT-TTF)$_2$X (X = IBr$_2$, I$_2$Br) at 4.2 K for several field angles ϕ measured from the b-axis. Panels (a) and (b) are results for the IBr$_2$ and I$_2$Br salts, respectively. The square of the inter-layer resistance normalized by the inter-layer resistance at zero field is plotted versus the square of the field. The inset of (a) shows FS of these materials obtained from AMRO [3]. Experimental configuration of the transverse MR is shown in the inset of (b).

4. Distribution of τ on FS derived from the inter-layer transverse MR results

To estimate the distribution of τ on FS, we start from the general Chambers expression of the inter-layer transverse MR for a q2D system [4, 18, 19]

$$\frac{R_\perp(B,\phi)}{R_\perp(0)} = \frac{I_0}{I}, \tag{2}$$

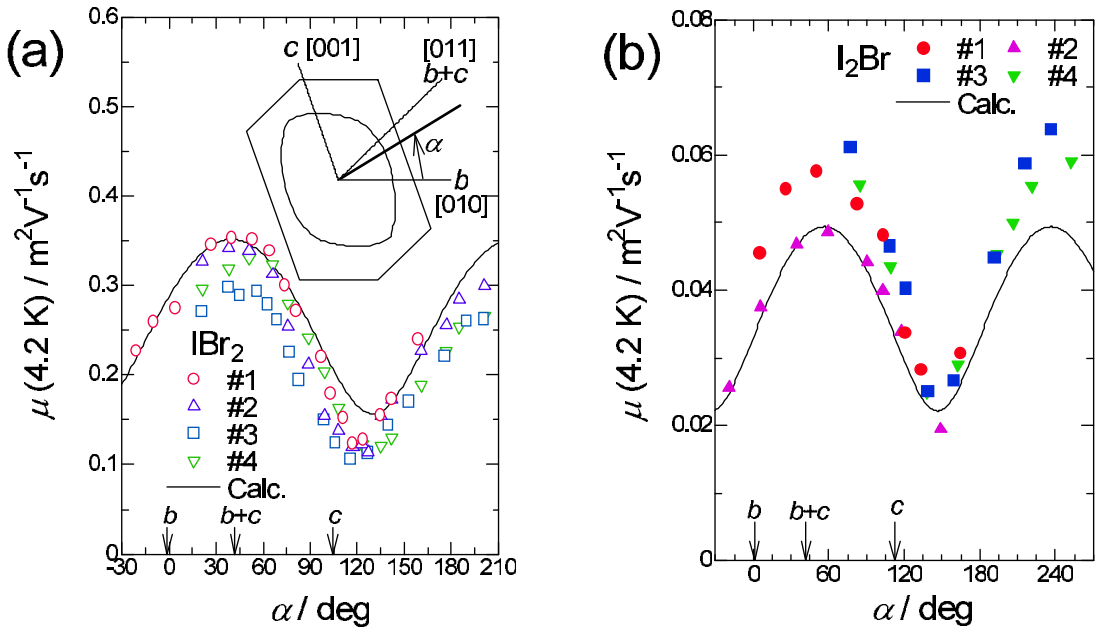

Figure 3. In-plane mobility at 4.2 K for the IBr_2 salt (a) and the I_2Br salt (b). The in-plane angle α is measured from the b-axis as shown in the inset of panel (a). In each figure, data are plotted for four samples. The solid curves are the simulations based on equation (7) by use of τ in figure 4.

where

$$I_0 = \oint_{\mathrm{FS}} \rho(k)\tau(k)\,\mathrm{d}k \tag{3}$$

and

$$I = \oint_{\mathrm{FS}} \rho(k)\tau(k)\frac{1}{1+[a_\perp e\tau(k)|\boldsymbol{v}(k)\times\boldsymbol{B}|/\hbar^2]^2}\,\mathrm{d}k. \tag{4}$$

We introduce here the k-local (differential) density of states (DOS) $\rho(k)$, satisfying,

$$D_{\mathrm{F}} = \oint_{\mathrm{FS}} \rho(k)\,\mathrm{d}k, \tag{5}$$

where D_{F} denotes the 2D DOS per single spin. Note that $\rho(k)$ is expressed using $\boldsymbol{v}(k)$ as

$$\rho(k) = \frac{1}{4\pi^2\hbar|\boldsymbol{v}(k)|}. \tag{6}$$

The contour integrations are taken over the 2D closed FS. The parameter $a_\perp$ is the inter-layer spacing, $\boldsymbol{v}(k)$ and $\tau(k)$ are the Fermi velocity and the lifetime at k-point, respectively, and $\boldsymbol{B} = B(\cos\phi, \sin\phi)$. It is assumed that $\tau(k)$ is independent of B. The inter-layer transverse MR of $Tl_2Ba_2CuO_6$ was numerically calculated by the use of equations (2)–(6) assuming uniform τ on FS, which agreed with the experimental transverse MR under low field [20]. In this case, we concentrate our attention on $\boldsymbol{k}$-dependent dynamics in connection with the anisotropic mobilities in the low-field regime, rather than the field dependence. For this purpose, we take account of the $\boldsymbol{k}$-dependence of τ on FS, as in the following. If the field is not too high, equation (2) is reduced into a simple form of equation (1), in terms of the averaged mobility μ_α as defined by

$$\mu_\alpha^2 = C\oint_{\mathrm{FS}} \rho(k)\tau(k)\,|\tau(k)\boldsymbol{v}(k)\times\mathbf{u}_B(\phi)|^2\,\mathrm{d}k, \tag{7}$$

where $\mathbf{u}_B(\phi)$ is the unit vector pointing in the field direction, and the factor C is

$$C = 2(a_\perp e/\hbar)^2/\oint_{\mathrm{FS}} \rho(k)\tau(k)\,\mathrm{d}k. \tag{8}$$

For a 2D cylindrical FS of a parabolic band, $E = \hbar^2(k_x^2 + k_y^2)/2m^*$; with constant τ, equation (8) yields a well-known formula for the mobility, i.e. $\mu = |e|\tau/m^*$. Equation (7) means that $\mu(\alpha)^2$ is given by the average of the α-component of $\tau(k)^2\boldsymbol{v}_{\mathrm{F}}(k)^2$ weighted with $\rho(k)\tau(k)$ over FS.

The Fermi velocity, $\boldsymbol{v}_{\mathrm{F}}(\boldsymbol{k}) = \hbar^{-1}\mathrm{grad}_{\boldsymbol{k}}\,E$, can be calculated from the band structure and FS. A tight-binding band is available for β-(BEDT-TTF)$_2$IBr$_2$ [13]. It is written as

$$E_\pm(\boldsymbol{k}) = 2t_{\mathrm{r}}\cos(\boldsymbol{k}\cdot\boldsymbol{c}) \pm \sqrt{E_1^2 + E_2^2}, \tag{9}$$

$$E_1 = t_{\mathrm{p1}}\cos[(\boldsymbol{k}\cdot\boldsymbol{b}+\boldsymbol{k}\cdot\boldsymbol{c})/2] + t_{\mathrm{q1}}\cos[(\boldsymbol{k}\cdot\boldsymbol{b}-\boldsymbol{k}\cdot\boldsymbol{c})/2], \tag{10}$$

$$E_2 = t_{\mathrm{p2}}\sin[(\boldsymbol{k}\cdot\boldsymbol{b}+\boldsymbol{k}\cdot\boldsymbol{c})/2] + t_{\mathrm{q2}}\sin[(\boldsymbol{k}\cdot\boldsymbol{b}-\boldsymbol{k}\cdot\boldsymbol{c})/2]. \tag{11}$$

For experimental consistency, the transfer integral parameters appearing here should be set to give FS in agreement with the AMRO result. We find the parameter set, $t_{\mathrm{r}}/t_{\mathrm{p1}} = 0.056$, $t_{\mathrm{p2}}/t_{\mathrm{p1}} = 0.111$, $t_{q1}/t_{p1} = 0.361$, $t_{\mathrm{q2}}/t_{\mathrm{p1}} = 0.007$ and $E_{\mathrm{F}}/t_{\mathrm{p1}} = 0.607$, to satisfactorily reproduce FS deduced from AMRO of this material. The reproduced FS is depicted in figure 4(b) in comparison with the AMRO

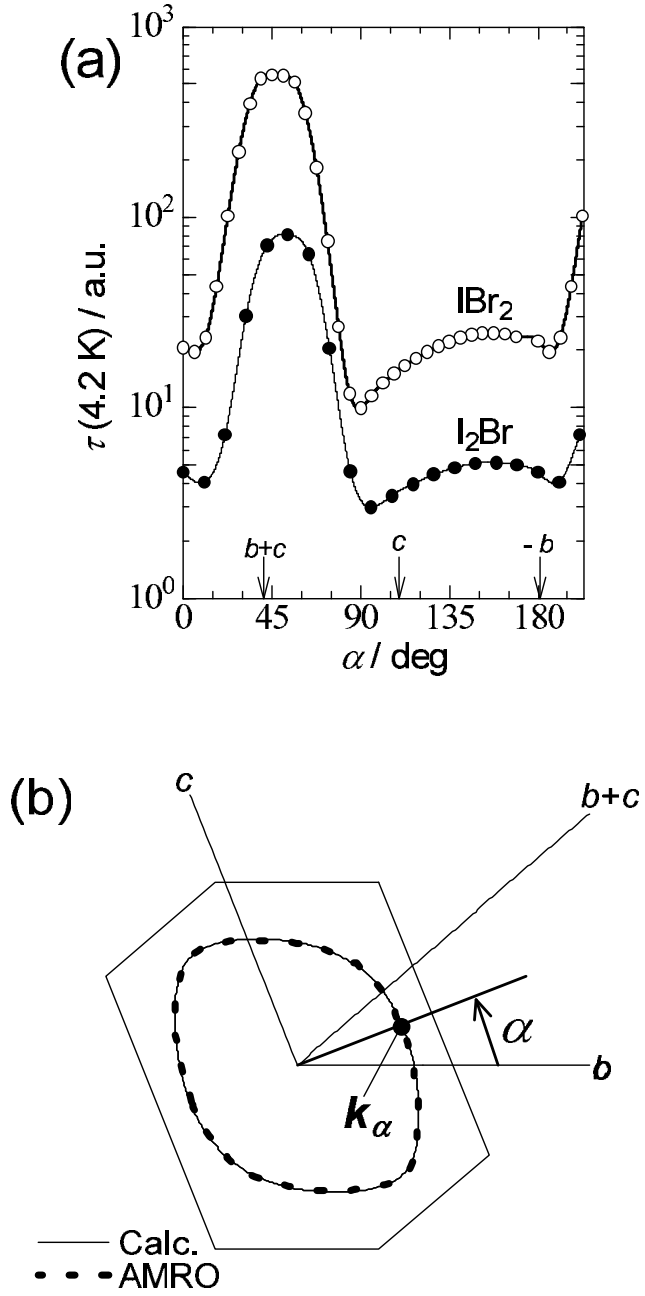

Figure 4. (a) Angle dependence of the lifetime $\tau(\alpha)$ for the IBr_2 and I_2Br salts. The curves are drawn to guide the eyes. (b) The FS deduced from AMRO [3] is compared with the reproduced FS by equation (9) using the parameters, $t_r/t_{p1} = 0.056$, $t_{p2}/t_{p1} = 0.111$, $t_{q1}/t_{p1} = 0.361$, $t_{q2}/t_{p1} = 0.007$ and $E_F/t_{p1} = 0.607$. The Fermi energy measured from the upper band energy at $\boldsymbol{k} = 0$ is $[E_F - (2t_r + t_{p1} + t_{q1})]/t_{p1} = -1.406$. The relation between α and k_α on the FS is also shown.

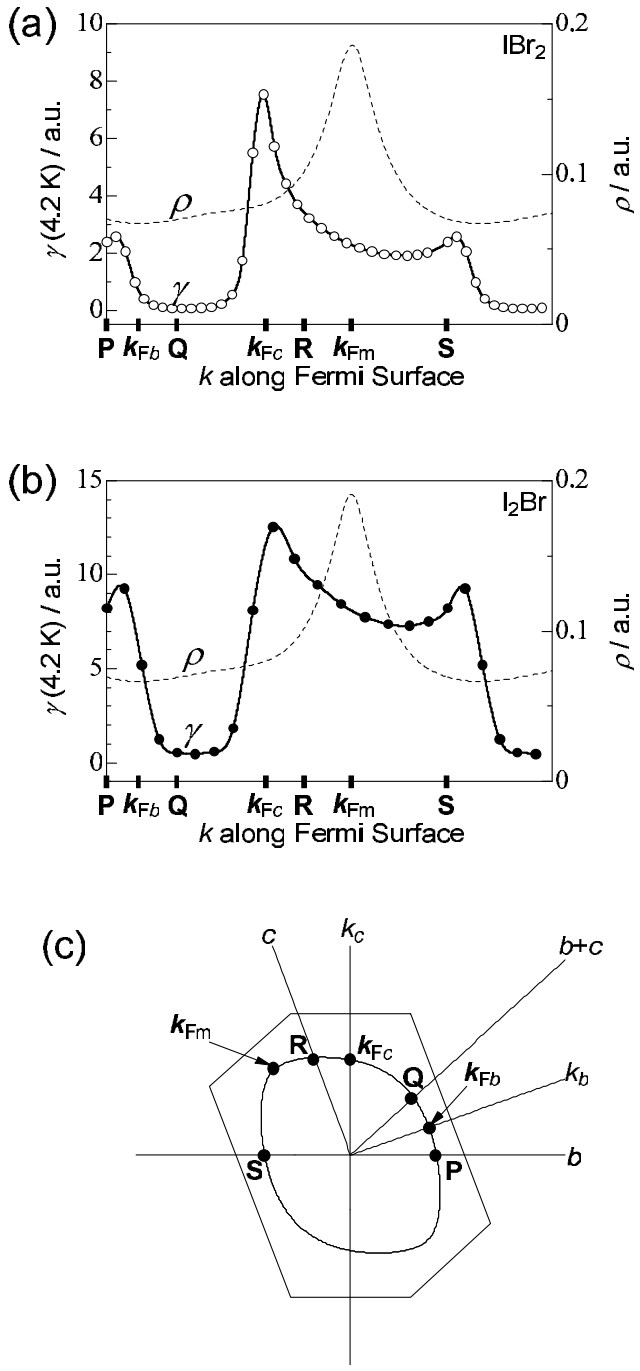

Figure 5. Scattering rate γ at each k-point on FS for the IBr_2 salt (a) and the I_2Br salt (b). The curves are drawn to guide the eyes. Dashed curves show the k-local DOS ρ. Some k-points on the k-axis in (a) and (b) are depicted on the FS in (c).

result. Note that only relative values can be determined for these energy parameters and Fermi velocities. As regards the standard value, $t_{p1} = 0.245$ eV was reported for β-(BEDT-TTF)$_2$I$_3$ [21]. Taking account of the similarity between the two salts, we assume the same band structure for the I_2Br salt as an approximation.

Then it is possible to simulate μ_α for the assumed distribution of $\tau(k)$ on FS. Our purpose is to find the τ values that reproduce the observed μ_α behaviour. To this end, we parameterized τ at the selected k_α-points in the range $0 \leqslant \alpha \leqslant \pi$ on FS as shown in figure 4. We have a set of equations (7) for 30 μ_α data for sample #1 of the IBr_2 salt or 20 for sample #2 of the I_2Br salt (figure 3). Solving this numerically, we have found a set of $\tau(\alpha)$ values that agree well with the observed μ_α as shown by the solid curves in figure 3. The distribution of τ thus estimated is shown in figure 4. As well as the transfer integrals and the Fermi velocities, the τ values shown here are relative ones. The two salts exhibit similar features of the τ distribution. Pronounced dip structures appear around

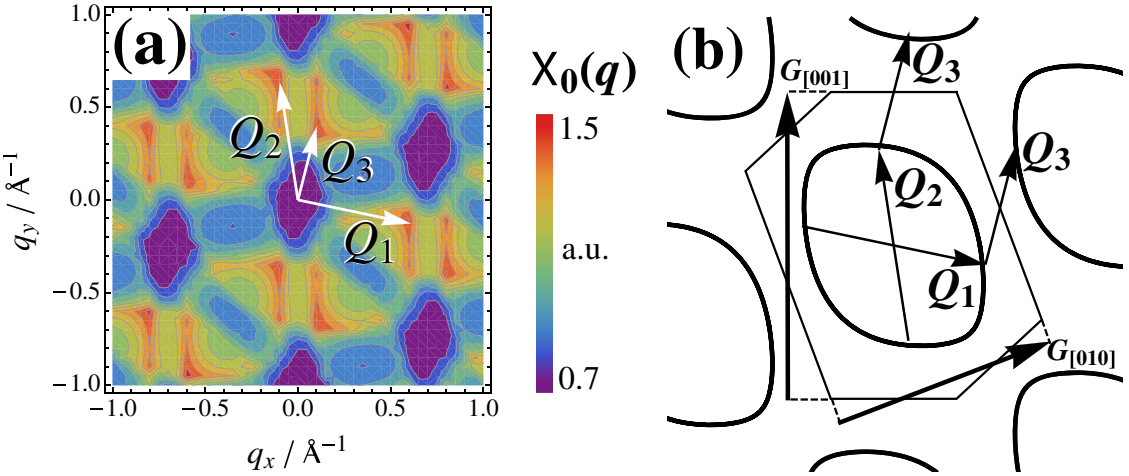

Figure 6. (a) Contour plot of the susceptibility $\chi_0(\boldsymbol{q})$ in arbitrary units mapped onto $\boldsymbol{q}$ space. Peaks are found at $\boldsymbol{Q}_1$, $\boldsymbol{Q}_2$ and $\boldsymbol{Q}_3$. (b) Relation between these three vectors and FS. FSs are shown in the extended zone. $\boldsymbol{G}_{[010]}$ and $\boldsymbol{G}_{[001]}$ are reciprocal lattice vectors.

$\alpha = -6^\circ$ and 90° accompanied by a small curvature of FS. The non-uniform distribution of τ thus found is likely to explain the observed anisotropy of μ.

The present method is applicable when field dependence of equation (1) is observed and reliable data on the band structure are available. If relation (1) is broken, the inter-layer TMR should be analysed exactly by the use of equations (2)–(6).

5. Discussion

Let us next examine the origin of the anomalously short lifetime on the specific k-points on FS. Scattering rate $\gamma(k) = 1/\tau(k)$, rather than τ, is more conveniently referred to for this purpose. In figure 5, $\gamma(k)$ is plotted versus k travelling along FS. Also plotted is the k-local DOS $\rho(k) = 1/4\pi^2\hbar|\boldsymbol{v}(k)|$, showing a peak at $\boldsymbol{k}_{\rm Fm}$ near the c-direction. This enhancement of $\rho(k)$ comes from the close spacing between FS and the zone boundary. The anisotropy of $\rho(k)$ is less significant; it varies within the range by a factor of about 2. If (quasi-)elastic forward scatterings due to impurities or long-wavelength acoustic phonons are predominant, $\gamma(k)$ is designated by $\rho(k)$. However, such a usual scattering cannot explain the present results, as is apparent from figure 5.

We have to go further, taking into account the scattering involving two carriers on FS. Such scattering with momentum exchange between $\hbar\boldsymbol{k}_{\rm F}$ and $\hbar\boldsymbol{k}'_{\rm F}$ is related to fluctuations of wavenumber $\boldsymbol{q} = \boldsymbol{k}'_{\rm F} - \boldsymbol{k}_{\rm F}$. To search $\boldsymbol{q}$ relevant to the peculiar carrier dynamics on FS, we have carried out the calculations of the susceptibility, $\chi_0(\boldsymbol{q})$, which describes the dynamical response of the system to $\boldsymbol{q}$-fluctuation (correlation). It is given by the standard expression

$$\chi_0(\boldsymbol{q}) = -\frac{1}{2\pi^2}\int\int_{\rm 1st.B.Z.} \frac{f(E_{\boldsymbol{q}+\boldsymbol{k}}, T) - f(E_{\boldsymbol{k}}, T)}{E_{\boldsymbol{q}+\boldsymbol{k}} - E_{\boldsymbol{k}}}\,{\rm d}k_b\,{\rm d}k_c, \tag{12}$$

where f is the Fermi distribution at temperature T, $E_{\boldsymbol{k}}$ is the band energy and the integration is taken over the first Brillouin zone. Using $k_{\rm B}T/t_{\rm p1} = 0.0069$, $\chi_0(\boldsymbol{q})$ is mapped onto the $\boldsymbol{q}$ space, as shown in figure 6(a). This temperature, corresponding to $T = 20$ K for the cited value $t_{\rm p1} = 0.245$ eV, is slightly larger than the smearing of FS, $\gamma/k_{\rm B} \approx 10$ K. The peaks of $\chi_0(\boldsymbol{q})$, indicated by the red-coloured areas in the map, are the so-called 'hot spots', which designate the candidate $\boldsymbol{q}$ of relevance. We find that $\boldsymbol{Q}_1$, $\boldsymbol{Q}_2$ and $\boldsymbol{Q}_3$ yield notable peaks of $\chi_0(\boldsymbol{q})$. They are related to FS as in figure 6(b). The anomalous enhancement of $\gamma(k)$ (figure 5) is now explainable in terms of the relevant $\boldsymbol{q}$. The most prominent peak of $\gamma(k)$ at $k_{\rm Fc}$ is related to $\boldsymbol{Q}_2$ and $\boldsymbol{Q}_3$, and the second peak to $\boldsymbol{Q}_1$. The k-local DOS ρ is enhanced near the zone boundary, so that it is sensitive to the distance between the portion of FS and the zone boundary. The prominent peak of γ related to $\boldsymbol{Q}_2$ of the IBr_2 salt may be overestimated due to less precise estimation of ρ around the anomalous peak at $k_{\rm Fm}$. On the other hand, the peak height near $\boldsymbol{Q}_2$ is comparable with that near $\boldsymbol{Q}_1$ for the I_2Br salt (figure 5(b)). The peak of ρ at $k_{\rm Fm}$ gives rise to high one-electron scattering rate, which is suggested to raise the tails of the two-electron contributions from $\boldsymbol{Q}_2$ and $\boldsymbol{Q}_1$. The origin of the broad part of high γ around $k_{\rm Fm}$ is qualitatively understandable in this way, although the quantitative detailed scattering mechanism is open for further theoretical study. Each of these vectors, $\boldsymbol{Q}_1$, $\boldsymbol{Q}_2$, $\boldsymbol{Q}_3$, links two $\boldsymbol{k}$-points on flat portions of FS, leading to partial $2\boldsymbol{k}_{\rm F}$ nesting of FS. Note that $\boldsymbol{Q}_3$ is related to $\boldsymbol{Q}_1$ and $\boldsymbol{Q}_2$ as $\boldsymbol{Q}_3 = \boldsymbol{G}_{[010]} - \boldsymbol{Q}_1 = \boldsymbol{G}_{[001]} - \boldsymbol{Q}_2$ in terms of the reciprocal lattice vectors $\boldsymbol{G}_{[010]}$ and $\boldsymbol{G}_{[001]}$. This suggests that these $2\boldsymbol{k}_{\rm F}$ modes of fluctuations are of potential importance in the transport properties of the β salts. It still remains to be elucidated which of the electron–phonon or electron–electron coupling drives the $2\boldsymbol{k}_{\rm F}$ modes.

This inter-layer transverse MR method will be applicable to general cases including phase transition. Even if deformation of FS is caused by transition, the analyses of transverse MR can be performed as far as reliable data on the deformation are available. Information on scattering obtained there yields deep insights into the origin of the transition.

6. Summary

The transverse MR experiments on layered organic conductors β-(BEDT-TTF)$_2$IBr$_2$ and β-(BEDT-TTF)$_2$I$_2$Br at 4.2 K provide the in-plane anisotropy of the mobility μ. From this, and the appropriate FS data based on the tight-binding model, the distribution of the lifetime τ on FS has been estimated. Anomalously suppressed τ on specific $\boldsymbol{k}$-points on FS is found and is likely to explain the observed anisotropy of μ. The transverse MR behaviour is thus shown to include information on the carrier dynamics on FS. The strong scattering on the specific $\boldsymbol{k}$-points on FS is related to $2\boldsymbol{k}_{\mathrm{F}}$-fluctuations with partial nesting of FS, as suggested by the peaks found in the $\chi(\boldsymbol{q})$ mapping.

Acknowledgments

We acknowledge Professor Takeo Kato for his stimulating and helpful discussions. We are grateful to Professor Seiichi Kagoshima for his enlightening comments and encouragement. We are grateful to the reviewer's helpful comments on the relation of the peak of γ and a specific $\boldsymbol{q}$. Experimental help by K Suzuki is also acknowledged. This work was partially supported by Grants-in-Aid for Scientific Research on Innovative Areas 'New Frontier of Materials Science Opened by Molecular Degrees of Freedom' (no. 21110519) from the Ministry of Education, Culture, Sports, Science and Technology.

References

[1] Kartsovnik M V, Kononovich P A, Laukhin V N and Shchegolev I F 1988 *JETP Lett.* **48** 541
[2] Kajita K, Nishio Y, Takahashi T, Sasaki W, Kato R, Kobayashi H, Kobayashi A and Iye Y 1989 *Solid State Commun.* **70** 1189
[3] Kartsovnik M V, Laukhin V N, Pesotskii S I, Schegolev I F and Yakovenko V N 1992 *J. Phys. I* **2** 89
[4] Lebed A G and Bagmet N N 1997 *Phys. Rev.* B **55** 8654
[5] Kontani H, Kanki K and Ueda K 1999 *Phys. Rev.* B **59** 14723
[6] Kontani H 2008 *Rep. Prog. Phys.* **71** 026501
[7] Jindo R, Sugawara S, Tajima N, Yamamoto H M, Kato R, Nishio Y and Kajita K 2006 *J. Phys. Soc. Japan* **75** 013705
[8] Sugawara S, Ueno T, Tajima N, Nishio Y and Kajita K 2007 *J. Phys. Soc. Japan* **76** 114706
[9] Konoike T, Fujiwara H, Zhang B, Kobayashi H, Nishimura M, Yasuzuka S, Enomoto K and Uji S 2004 *Physica* C **412–414** 107
[10] Kobayashi H, Tomita H, Naito T, Kobayashi A, Sakai F, Watanabe T and Cassoux P 1996 *J. Am. Chem. Soc.* **118** 368
[11] Fujiwara H, Fujiwara E, Nakazawa Y, Narymbetov B Z, Kato K, Kobayashi H, Kobayashi A, Tokumoto M and Cassoux P 2001 *J. Am. Chem. Soc.* **123** 306
[12] Williams J M, Wang H H, Beno M A, Emage Y J, Sowa L M, Copps P T, Behroozi F, Hall L N, Carlson K D and Crabtree G W 1984 *Inorg. Chem.* **23** 3839
[13] Kobayashi H, Kato R, Kobayashi A, Saito G, Tokumoto M, Anzai H and Ishiguro T 1985 *Chem. Lett.* **14** 1293
[14] Tokumoto M, Anzai H, Bando H, Saito G, Kinoshita N, Kajimura K and Ishiguro T 1985 *J. Phys. Soc. Japan* **54** 1669
[15] Bulaevskii L N, Ginodman A V, Gudenko M V, Kartsovnik M V, Kononovich P A, Laukhin V N and Shchegolev I F 1988 *Sov. Phys.—JETP* **67** 810
[16] Kartsovnik M V, Kononovich P A, Laukhin V N, Pesotskii V N and Shchegolev I F 1990 *JETP Lett.* **70** 735
[17] Kartsovnik M V 2004 *Chem. Rev.* **104** 5737
[18] Chambers R G 1952 *Proc. Phys. Soc.* A **65** 458
[19] Schofield A J and Cooper J R 2000 *Phys. Rev.* B **62** 10779
[20] Dragulescu A, Yakovenko V M and Singh D J 1999 *Phys. Rev.* B **62** 6312
[21] Tajima H, Yakushi K, Kuroda H and Saito G 1985 *Solid State Commun.* **56** 159